VOL. 6, NO. 3, MARCH 2011 ISSN 1819-6608
ARPN Journal of Engineering and Applied Sciences

www.arpnjournals.com

VOLTAGE SAG INFLUENCE ON FATIGUE LIFE OF THE DRIVETRAIN OF FIXED SPEED WIND TURBINES

Badrinath V.[1], D. Santos-Martin[2] and H. M. Jensen[1]
[1]Aarhus School of Engineering, Aarhus University, Dalgas Avenue, Aarhus C, Denmark
[2]Department of Electrical Engineering, University Carlos III Madrid, Spain
E-Mail: vb@agse.dk

ABSTRACT

Occurrence of voltage sags due to electrical grid faults and other network disturbances generate transients of the generator electromagnetic torque which result in significant high stresses and noticeable vibrations for the wind turbine mechanical system and may also have a detrimental effect on the fatigue life of important drivetrain components. The high penetration of wind energy in the electrical grids demands new requirements for the operation of wind energy conversion systems. Although fixed speed wind turbine technology is nowadays replaced by variable speed wind turbines. In some countries (Spain and Germany) with high wind energy penetration it is mandatory or under bonus to retrofit these fixed speed wind turbines and provide ride through capability. An electro-mechanical model is built to simulate the grid disturbances that easily excite the asynchronous generators poorly damped by the stator flux oscillations which cause high transients of the generator electromagnetic torque. This paper focuses in estimating the resulting significant stresses transients due to the electromagnetic torque transients, which transmits to the wind turbine mechanical system that may have a detrimental effect on the fatigue life of drivetrain components. The capability to simulate these phenomena is a novel aspect in the present effort.

Keywords: model, voltage sag, wind turbines, drivetrain, fatigue life, asynchronous generator, wind energy conversion system.

INTRODUCTION

Due to increasing environmental consciousness, renewable energy has regained interest. Among the several renewable energy sources being explored, wind energy is one of the promising sources. The wind industry, in particular, has seen an unquenchable demand as a result, and the need for reliable and affordable wind turbines now is all the more apparent. Unfortunately, recurrent drivetrain failures have characterized the industry and have prevented turbines in achieving their intended 20-year design life. The component most responsible for downtime is the gearbox [1]. Gearbox replacement and lubrication account for 38% of the parts cost for the entire turbine system [2]. This situation calls for the implementation of new and advanced simulation techniques to be integrated into the gearbox-design process so that this component can meet its intended design life.

In many countries like Germany, Spain, etc., new grid codes have been established [3, 4, 5] demanding new wind farms to behave as conventional power plants. One of the main requirements established in these new grid codes is the so-called wind turbine low voltage ride through (LVRT) capability. This specification aims to improve transient stability in a power system with a high penetration of wind energy by guarantying that the wind turbine remains connected when voltage disturbances appear while satisfying certain reactive power requirements. This LVRT requirement is well established for the new variable speed wind turbines equipped with power electronic converters but recently due to the high wind energy penetration in some countries is being applied to older fixed speed wind turbines (FSWT) as shown in Figure-1 like in Spain or Germany what implies to retrofit them to provide the LVRT capability. Most of the studies concerning LVRT have been focused on the electrical or control systems while neglecting or simplifying the mechanical components. Unfortunately grid disturbances easily excite the asynchronous generators poorly damped stator flux oscillations which develops the transients in electromagnetic torque that affect the whole drive train components.

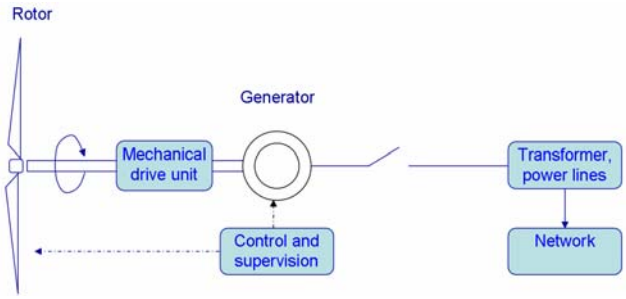

Figure-1. Simulation structure of the fixed speed wind turbine system with active stall.

Considerable research has been done on ride-through capability of wind turbines. Most of this research, however, has been done using relatively simple mechanical and aerodynamic models of wind turbines that neglect a number of significant characteristics from mechanical point of view. It is very important to study both the electrical and mechanical aspects of wind turbines simultaneously, since an electrical network disturbance such as voltage sag can affect mechanical performance by the torque transients which may have a detrimental effect on the fatigue life.

Since the aim of the study is to simulate the impact of the voltage sag impact on the detrimental effect on the fatigue life of drivetrain components under various operating conditions. A computational model was built in MATLAB/Simulink [6] environment which contains the detailed electrical and mechanical systems of a wind turbine. This computation model is expected to provide the overall accuracy needed during the design, development, testing, and deployment by considering the interaction aspects of the Wind turbine system in response to the voltage sags during the grid disturbances.

WIND TURBINE MODEL DESCRIPTION

Generator modeling

Applying the standard modeling assumptions of linearity to the magnetic circuits and sinusoidal distributed stator windings, the general complex vector model of an induction machine (IM) in the synchronous reference frame can be expressed as:

$$\begin{aligned}\overline{u_s} &= R_s\overline{i_s} + \frac{d\overline{\phi_s}}{dt} + j\omega_s\overline{\phi_s}\\ 0 &= R_r\overline{i_r} + \frac{d\overline{\phi_r}}{dt} + js\omega_s\overline{\phi_r}\\ \overline{\phi_s} &= L_s\overline{i_s} + L_m\overline{i_r}\\ \overline{\phi_r} &= L_m\overline{i_s} + L_r\overline{i_r}\end{aligned} \quad (1)$$

where u_s is the stator voltage; i_s and i_r are the stator and rotor currents; φ_s and φ_r are the stator and rotor flux linkages; L_s, L_r are the stator and rotor and inductance; L_{ds}, L_{dr} are the stator and rotor leakage inductance; R_s, R_r are the stator and rotor resistances, respectively; ω_s is the grid pulsation and s the slip parameter.

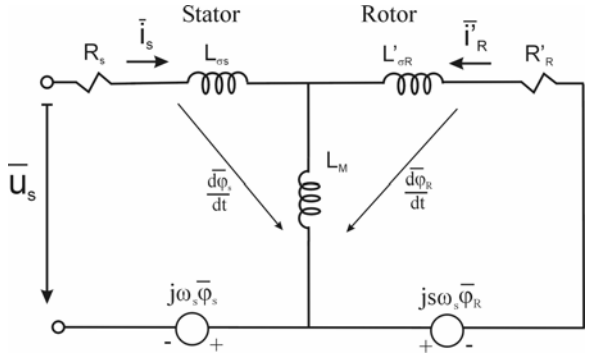

Figure-2. Induction Machine equivalent circuit of the dynamic model in asynchronous reference frame (d-q).

This model can be written in the following matrix form:

$$\begin{aligned}\frac{d}{dt}\begin{bmatrix}\overline{\phi_s}\\ \overline{\phi_r}\end{bmatrix} &= -\begin{bmatrix}R_s & 0\\ 0 & R_r\end{bmatrix}\begin{bmatrix}\overline{i_s}\\ \overline{i_r}\end{bmatrix} - j\omega_s\begin{bmatrix}1 & 0\\ 0 & s\end{bmatrix}\begin{bmatrix}\overline{\phi_s}\\ \overline{\phi_r}\end{bmatrix} + \begin{bmatrix}\overline{u_s}\\ 0\end{bmatrix}\\ \begin{bmatrix}\overline{i_s}\\ \overline{i_r}\end{bmatrix} &= \begin{bmatrix}L_s & L_m\\ L_m & L_r\end{bmatrix}^{-1}\begin{bmatrix}\overline{\phi_s}\\ \overline{\phi_r}\end{bmatrix}\end{aligned} \quad (2)$$

As each complex equation stands for two real ones, this vector form can be expanded easily. These algebraic-differential equations (2) can be expressed as a state variable model of fluxes (3) with U as an exogenous or perturbation variable:

$$\frac{d}{dt}\Psi = A_\phi(t)\Psi + U \quad (3)$$

The homogeneous time varying linear system associated to (5) is:

$$\frac{d}{dt}\Psi = A_\phi(t)\Psi \quad (4)$$

The time-variant and complex coefficients matrix A_φ can be approximated by:

$$A_\phi = \begin{bmatrix}\frac{-R_sL_r}{\sigma L_sL_r} - j\omega_s & \frac{R_sL_m}{\sigma L_sL_r}\\ \frac{R_rL_m}{\sigma L_sL_r} & \frac{-R_rL_s}{\sigma L_sL_r} - js\omega_s\end{bmatrix} \approx \begin{bmatrix}-\frac{R_s}{2L_d} - j\omega_s & \\ & \frac{R_r}{2L_d}\end{bmatrix} \quad (5)$$

Where L_d is the average value of stator and rotor leakage inductances? When substituting the stator and rotor resistances by an average value R the matrix A_φ can be again approximated by:

$$A_\phi \approx \begin{bmatrix}-\frac{R}{2L_d} - j\omega_s & \frac{R}{2L_d}\\ \frac{R}{2L_d} & -\frac{R}{2L_d} - js\omega_s\end{bmatrix} \quad (6)$$

The asynchronous generator dynamics can be characterized by the time-varying linear model (5) in the homogeneous form or by (3) when considering disturbances.

This model can be linearized at the equilibrium point ψ_0, and being considered, locally, as a time-invariant system (7).

$$\frac{d}{dt}\Psi = \left(A_\phi\right)_{\Psi 0}\Psi = A_{\phi 0}\Psi \quad (7)$$

Dynamic analysis

The solution to equation (7) can be developed in terms of the known state-transmission matrix that in this case takes the form of the matrix exponential function in the time domain and when using the Laplace transform yields in:

$$\Psi(t) = e^{A_{\phi 0} \cdot t} \Psi(0)$$

$$\Psi(s) = \left(sI - A_{\phi 0}\right)^{-1} \Psi(0) = \frac{adj(sI - A_{\phi 0})}{\left|sI - A_{\phi 0}\right|} \Psi(0) \quad (8)$$

The roots of the characteristic equation $\left|sI - A_{\varphi 0}\right|$, called also Eigen values of the homogeneous system or poles of the transfer function within the frequency-domain, characterizes locally the dynamic behavior of (7). From (6, 7) calculating the roots of $\left|\lambda I - A_{\varphi 0}\right|$ it can be proved that the eigen values of the system can be approximated by the diagonal terms of the matrix:

$$\lambda_1 \approx -\frac{R}{2L_d} - j\omega_s$$

$$\lambda_2 \approx -\frac{R}{2L_d} - js\omega_s \quad (9)$$

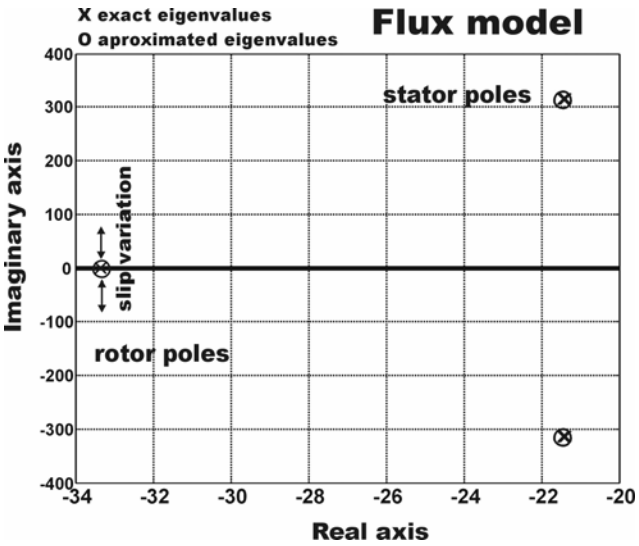

Figure-3. Example of poles location of the linearized induction machine model while changing the slip parameter.

The stator of the IM is directly coupled to the grid and unfortunately any grid disturbance easily excites the poorly damped stator flux poles (Figure-3).

The electromagnetic torque T_e of the generator is a scalar value [7] which dynamics depend only on the stator and rotor flux, being given by (9) and shown by Figure-3 that the former are poorly damped:

$$T_{elec} = \frac{3}{2} P_p \frac{L_m}{\sigma L_S L_R} \left|\overline{\phi_R} \wedge \overline{\phi_S}\right| = \frac{3}{2} P_p \frac{L_m}{\sigma L_S L_R} \mathrm{Im}(\overline{\phi_R}^* \cdot \overline{\phi_S}) \quad (10)$$

Where P_p the number of the generator pole is pairs; Im is the imaginary part of the scalar product of the two vectors and leakage coefficient is $\sigma = 1 - L_m^2 / (L_s L_r)$.

Drive train modeling

In the current investigation the source of disturbance is the generator torque due to the grid disturbances that caused the voltage sags and since the application of more sophisticated aeroelastic models are not used and the emphasis has been given more towards the study of detrimental effect on the life of gear box due to the network disturbances that causes the electromagnetic torque transients.

The aerodynamic torque on the drivetrain of a Wind Turbine (WT) varies continuously over the time due to the proper unsteady and non-linear characteristics of the complex aerodynamics; this aerodynamic torque is made constant in the present study. The electrical generator runs in a relatively high speed compared to the aerodynamic rotor. In the drivetrain a low speed shaft (LSS) in the rotor side are connected to a high speed shaft (HSS) in the electrical generator side by using a gearbox. Real installations are continua with infinitely degrees of freedom, but a detailed investigation with a reduced number of DOF is, as a rule, entirely sufficient for analyzing dynamic behavior. Consequently, it is sensible to look at a mathematical model that reflects the relevant features of the real technical system as accurately as possible. Any restrictions on movement (linkages) between the bodies are realized with joints with specific properties. Such mechanical systems are described mathematically by coupled ordinary differential and algebraic equations.

Mathematical modeling of the drivetrain system

The representation of the drivetrain containing the gear box and an ideal rotor model is shown in Figure-4. In this model the next considerations were made: rotor, gears and LSS are rigid bodies and HSS is flexible.

The tangential velocity vector at the contact point for the first gear expressed in the base of the fixed reference frame N is:

$$\mathbf{v}_1^T = \boldsymbol{\omega}_1 \times \mathbf{r}_1 = \left\{\dot{q}_1(t)\hat{\mathbf{n}}_3\right\} \times \left\{r_1 \hat{\mathbf{n}}_1\right\} = \dot{q}_1(t) r_1 \hat{\mathbf{n}}_2 \quad (11)$$

Where $\dot{q}_1$ and r_1 are the angular velocity and the radius of the first gear.

The tangential velocity at the contact point for the second gear is expressed in the base N :

$$\mathbf{v}_2^T = \boldsymbol{\omega}_2 \times \mathbf{r}_2 = \left\{\dot{q}_2(t)\hat{\mathbf{n}}_3\right\} \times \left\{-r_2 \hat{\mathbf{n}}_1\right\} = -\dot{q}_2(t) r_2 \hat{\mathbf{n}}_2 \quad (12)$$

Where $\dot{q}_2$ and r_2 are the angular velocity and the radius of the second gear.

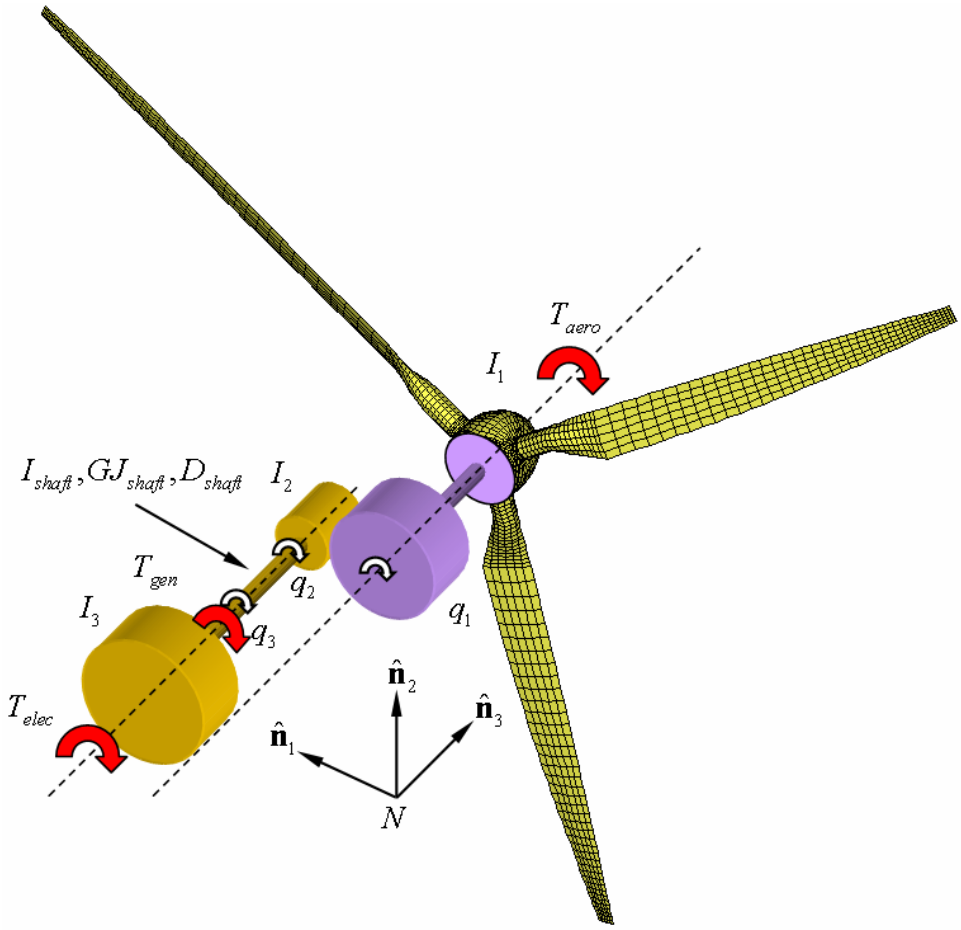

Figure-4. Dynamic representation of WT drivetrain.

At the contact point the tangential velocity must to be equal for both gears ($\mathbf{v}_1^T = \mathbf{v}_2^T$), and the constraint relation is:

$$\dot{q}_1(t) r_1 + \dot{q}_2(t) r_2 = 0 \rightarrow \dot{q}_2(t) = -n_g \dot{q}_2(t) \qquad (13)$$

where $n_g = r_1 / r_2$ is the gear ratio.

The kinetic energy for the system can be expressed as:

$$T = \frac{1}{2} I_1 \left[\dot{q}_1(t)\right]^2 + \frac{1}{2} I_2 \left[\dot{q}_2(t)\right]^2 + \frac{1}{2} I_3 \left[\dot{q}_2(t) + \psi(L)\dot{q}_3(t)\right]^2 + \frac{1}{2}\int_0^L I_{shaft}(\eta)\left[\dot{q}_2(t) + \psi(\eta)\dot{q}_3(t)\right]^2 d\eta \qquad (14)$$

Where $\dot{q}_3$ is the angular velocity spanned by the shape function ψ over all the shaft length? I_1, I_2 and I_3 are the rotational inertias for the rotor and gearbox, and the generator, respectively. And I_{shaft} is the shaft's rotational inertia distribution per unit length.

The potential energy for the system can be expressed as:

$$U = \frac{1}{2}\int_0^L GJ_{shaft}(\eta)\left[\psi'(\eta) q_3(t)\right]^2 d\eta \qquad (15)$$

Where GJ_{shaft} is the shaft's torsional stiffness distribution per unit length?

By using Lagrange's equations, virtual work principle for external and damping loads, the constraint relation and assuming $\psi(\eta) = \eta / L$ compatible with the shaft's boundary conditions relative to the rigid body movement and constant shaft's section and properties, the equations of motion for the system [8,9] are:

$$[\mathbf{M}]\{\ddot{\mathbf{q}}\} + [\dot{\mathbf{M}} + \mathbf{D}]\{\dot{\mathbf{q}}\} + [\mathbf{K}]\{\mathbf{q}\} = \{\mathbf{F}\} \qquad (16)$$

Where $\{\mathbf{q}\}$ is the configuration vector which contains the generalized coordinates, $[\mathbf{M}]$ is the mass matrix, $[\dot{\mathbf{M}}]$ is the first time derivative of the mass matrix, $[\mathbf{D}]$ is the

damping matrix, $[\mathbf{K}]$ is the stiffness matrix, and $\{\mathbf{F}\}$ is the vector of generalized forces. The intervening vectors and matrices in the equations of motion (16) are expressed in detail as below:

$$\{\mathbf{q}\} = \{q_1 \quad q_3\}^T \tag{17}$$

$$[\mathbf{M}] = \begin{bmatrix} I_1 + n_g^2\left(I_2 + I_3 + I_{shaft}L\right) & -n_g\left(I_3 + I_{shaft}L\right) \\ -n_g\left(I_3 + I_{shaft}L\right) & I_3 + I_{shaft}L \end{bmatrix} \tag{18}$$

$$\left[\dot{\mathbf{M}} + \mathbf{D}\right] = \begin{bmatrix} \dot{I}_1 & 0 \\ 0 & 0 \end{bmatrix} + \begin{bmatrix} 0 & 0 \\ 0 & D_{shaft} \end{bmatrix} = \begin{bmatrix} \dot{I}_1 & 0 \\ 0 & D_{shaft} \end{bmatrix} \tag{19}$$

$$[\mathbf{K}] = \begin{bmatrix} 0 & 0 \\ 0 & \dfrac{GJ_{shaft}}{L} \end{bmatrix} \tag{20}$$

$$\{\mathbf{F}\} = \begin{Bmatrix} T_{aero} - n_g T_{gen} \\ T_{gen} - T_{elec} \end{Bmatrix} \tag{21}$$

Where D is the HSS damping, T_{aero}, T_{gen} and T_{elec} are aerodynamical, generator and electromagnetic torques, respectively. And $\dot{I}_1$ is the first time derivative of I_1 which varies as the pitching angle of the blades changes.

TORQE TRANSIENTS IN THE DRIVETRAIN DURING THE THREE PHASE BALANCED VOLTAGE SAG

The voltage sag is characterized by the instantaneous drop in the magnitude of the generator torque due to an electrical grid failure, short circuits, overloads or starting of large motors and transformer energizing [10]. As a consequence, the pretension of the drive train is lost and large dynamic oscillations occur. These disturbances are usually named as low-frequency transients. The voltage sag events are chosen during the rated operating conditions in order to demonstrate the non-linear character of the torque transients' amplifications within the drivetrain.

STUDY CASE

The applications considered include faults. The emphasis is placed on the developed torque transients and their propagation up-stream of the drivetrain to study the impact of the over-current or over-voltage conditions that may arise for short durations of operation those are less harmful for squirrel-cage induction machines. The worst-case scenarios (faults electrically closest to the WT, minimum fault impedance, WT operating at rated power), are studied in order to assess the maximum stresses developed. For this reason, any protections of the WT (over-/under-voltage, over-/under-frequency, over-speed, over-current, phase unbalance) are also ignored, considering the WT fulfills the low voltage ride through capability. This is in accordance with [11], where "load cases" of simultaneous electrical and WT protection system faults are included.

Figure-5 presents the drivetrain torques for a chosen "voltage sag" event with a severity of 0.45 pu for a wind speed of 10m/s (rated power) shown in Figure-5(a). Figure-5(b) shows the normalized electromagnetic torque exhibits high transients during the voltage sag event. During the event a sustained torque oscillations are observed, due to the interaction of the air-gap magnetomotive forces (MMF), diminishing gradually. With current generator parameters used in the study (Appendix 1) shows maximum amplitude of 4.5 times the rated torque [12]. The propagation of the torque transients in the drivetrain is determined by its torsional characteristics. Due to consideration of the flexible shaft between the gearbox and the generator with a considerable damping the torque transients are not impacted as such in the up-stream. This transient is completely filtered out by the elasticity of the high-speed side before reaching the high-speed side of the drivetrain. Figure-5(c) shows the transients that are transmitted to the drivetrain upstream are still have a considerable impact. The drivetrain experiences a torque spike, approximately double the rated torque as shown in Figure-5(c), dying out in less than 100 ms., it is interesting to note, that the largest torque transients do occur during the voltage sag event that transmits from the flexible shaft to the drivetrain system. From Figure-5(b) and (c), it is the flexible shaft which is considered in the current simulation illustrates the reduction in the oscillations of the drivetrain significantly and mitigate fatigue damage to certain extent to the drivetrain. Still some of the oscillations transmit to the drivetrain system shown in Figure-5(d).

These torque transients that are detected numerically will provide a brief view on the detrimental effect of the fatigue life of the drivetrain due to voltage sags that arises during the network disturbances of the WT system during normal operations.

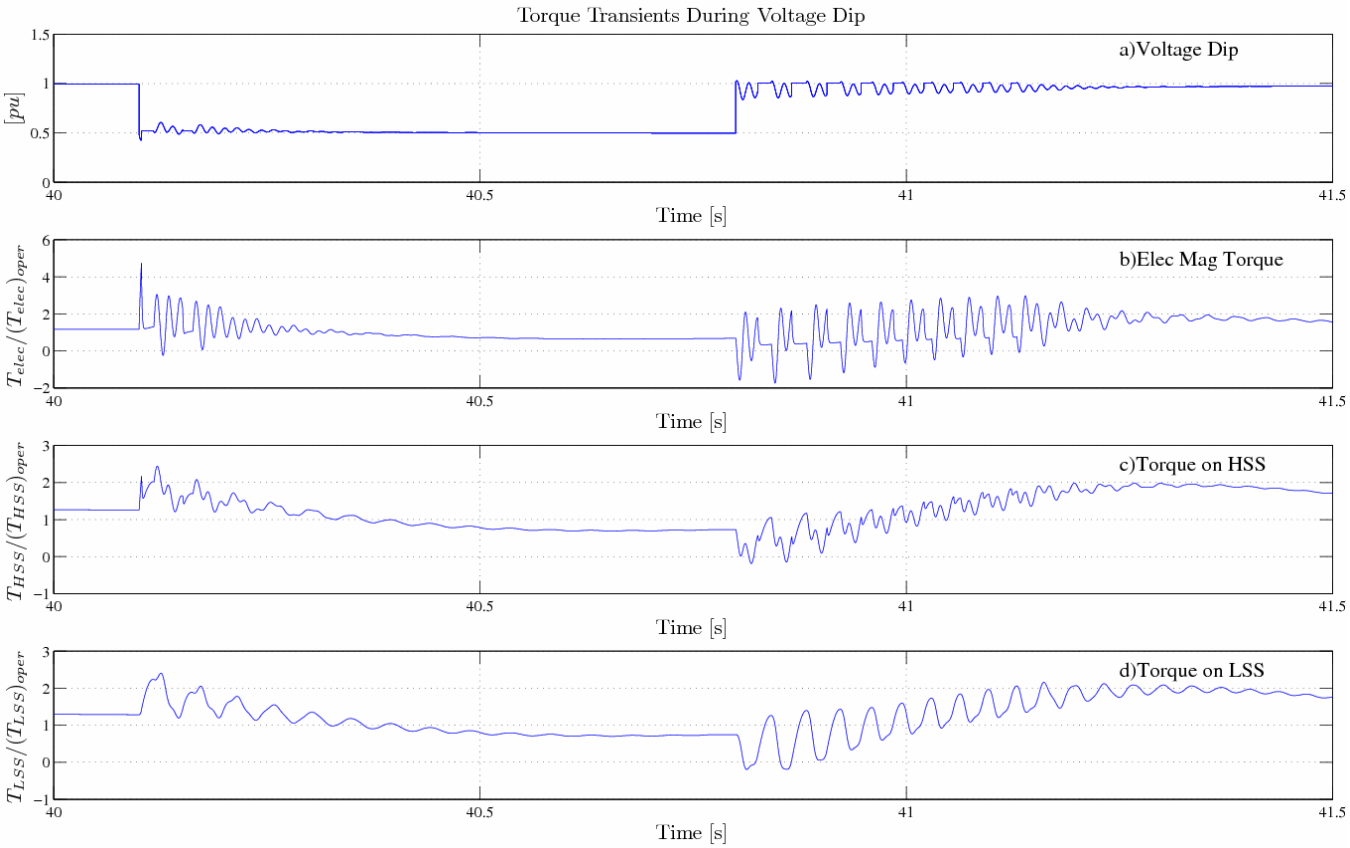

Figure-5. Network disturbance at wind speed 10 m/s with lowest phase voltage of 0.45 pu. (a) Voltage Sag event. (b) Torque on High-speed shaft. (c) Electromagnetic torque fluctuations. (d) Torque on Low-speed shaft.

FATIGUE EVALUATIONS

In widely used design practices of gearboxes, fatigue evaluations are based essentially on the time history of the Low-speed shaft torque on the rotor side. This practice of design is of only limited precision which may lead to the over-design or under-design of the components in the drivetrain system of the WT. It is very evident from the torque transients in the Figures 5 and 6. From the present study a better load spectra for the overall drivetrain system can be obtained, that can be later used in studying the detrimental effect of the fatigue life under unexpected service loading conditions viz. “voltage sags”. However, a novel approach is adopted in the present study that only estimates the correct load amplitudes seen by drivetrain as system, but not the associated load frequencies. This methodology can be implemented to estimate the component wise (Stage wise of the drivetrain system) loading history to have an accurate estimation of the detrimental effect on the life of the drivetrain system which is not in the interest of the present study.

Voltage sag occurrence

According to [13] the voltage sag frequency can be demonstrated by the number of events as a function of sag voltage in percent of nominal as shown in Figure-6, which describes the expected number of unsafe and troubling shutdowns as a function of voltage sensitivity.

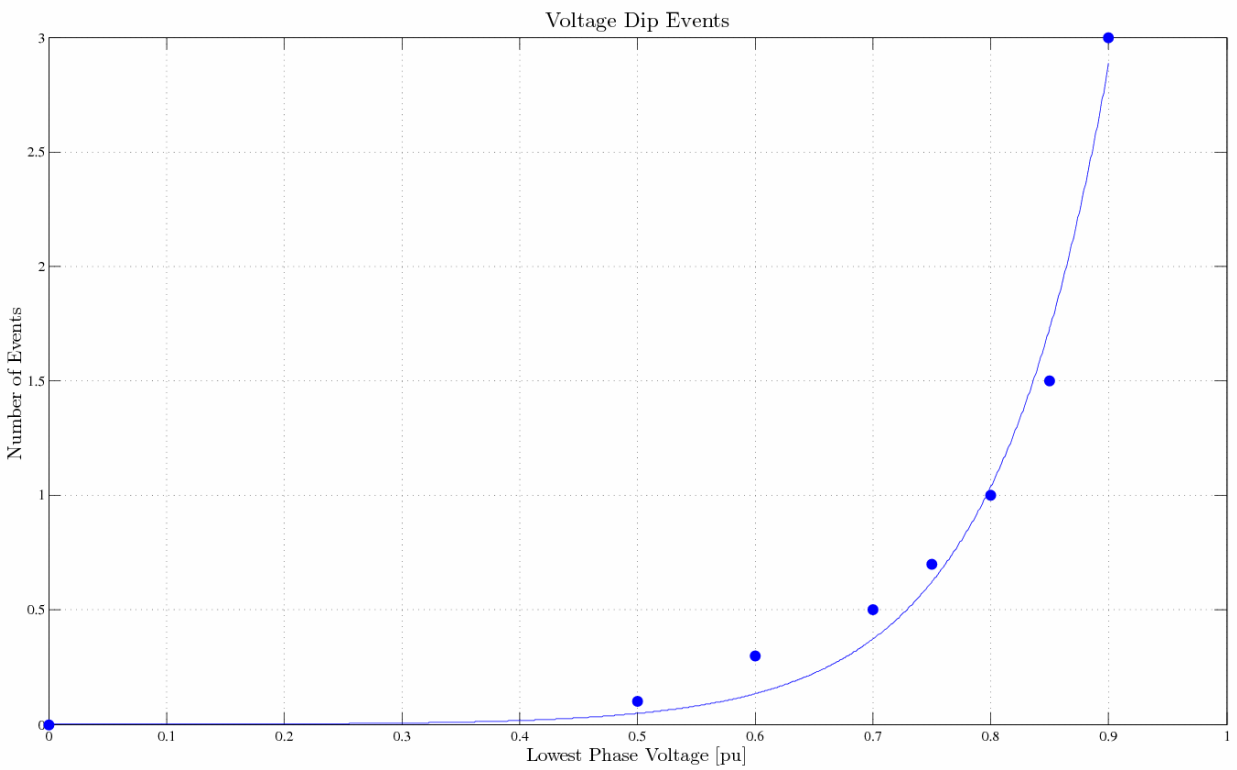

Figure-6. Number of events as a function of voltage sag magnitude.

In the present study it is considered a location with 10 events per year at 80 % of nominal voltage. This scenario is also considered in [13] and match with the contribution from each voltage system (345 kV, 230 kV, 138 kV, 69 kV) and for each of the form sag magnitude range (phase-to-ground, 2 phase-to-ground, phase-to-phase and 3 phase).

Estimating the detrimental effect on drivetrain's fatigue life

The loading spectrum on the low-speed side (rotor side) of the drivetrain is obtained by extracting Rain Flow Counting (RFC) of the overall loading history during the voltage sag event. Typical procedures used for fatigue life assessment under obtained random loadings on the drivetrain during the voltage sag event are implemented to perform this task. The estimated stress history from the random loading history as shown in Figure-7 is subjected to the rainflow cycle-counting method, which allows in determining the amplitudes and meaning values of counted cycles, their occurrence moment and time of duration as shown in Figure-8. Influence of the stress mean value was taken into consideration with the Marrow's stress-life characteristics [14].

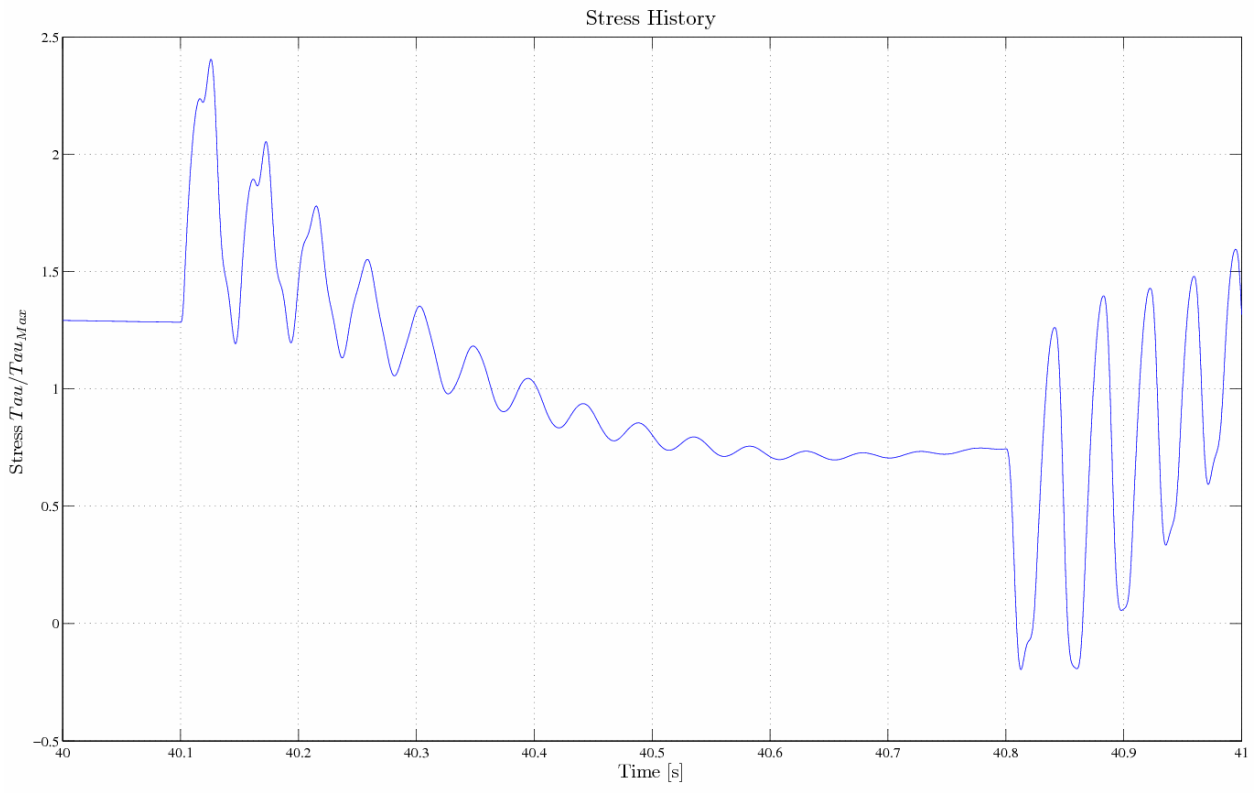

Figure-7. Stress history that are encountered during the voltage sag event.

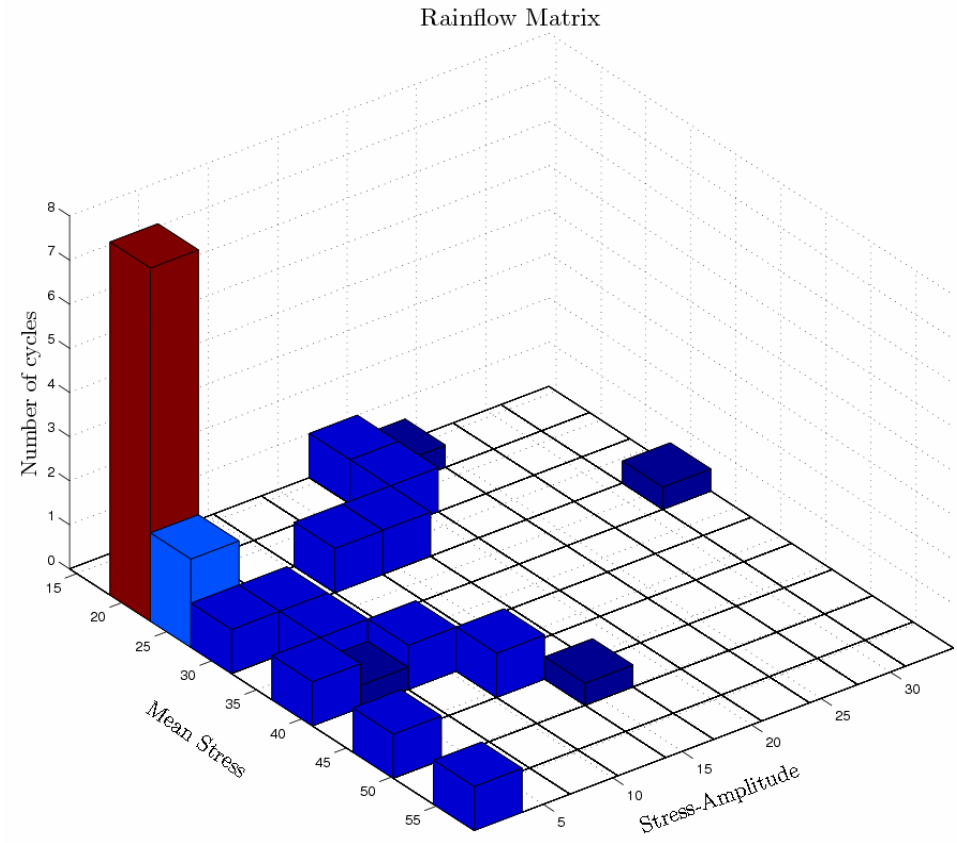

Figure-8. Estimated Rainflow matrix of the stresses registered during the voltage sag event.

On the assumption of the linear Palmgren-Miner hypothesis of damage accumulation and the stress-life fatigue characteristics of the material, the damage-time function was determined. The load segments, where the influence on the material fatigue was significant, were determined on the basis of the fixed damage-intensity level.

The mean and the amplitudes of the stress history (σ_{ai} and σ_{mi}) are estimated in order to calculate the damage D_i caused by the torque transients during the voltage event by the following equation.

$$D_i = \frac{n_i}{N_{fi}(\sigma_{ai}, \sigma_{mi})} \quad (22)$$

Where n_i is equal to 1 for a cycle and 0.5 for a half cycle, $N_{fi}(\sigma_{ai}, \sigma_{mi})$ is the function returning a number of cycles to failure according to the amplitude σ_{ai} and the mean value σ_{mi} that form the determined stress cycle and the fatigue characteristics of the material which can estimated by well known Marrow stress-life characteristics.

$$\sigma_a = \left(\sigma_f^{'} - \sigma_m\right)\left(2N_f\right)^b \quad (23)$$

$$N_{fi} = \frac{1}{2}\left(\frac{\sigma_{ai}}{\sigma_f^{'} - \sigma_{mi}}\right)^{1/b} \quad (24)$$

Where $\sigma_f^{'}$ the fatigue strength coefficient and b is the fatigue strength exponent.

To distinguish the amplitude and the mean values of the random history the cycle count is performed at the time of voltage sag event T_0 which is fixed time interval. Computation of the fatigue damage caused by the considered loading interval T_0 is usually realized with the assumption of hypothesis of the linear fatigue damage accumulation. The widely used Palmgren–Miner hypothesis assumes that the total damage occurred per voltage sag event can be expressed as the sum of particular damages caused by distinguished cycles as shown in Figure-9.

$$D = \sum_{i=1}^{k} D_i \quad (25)$$

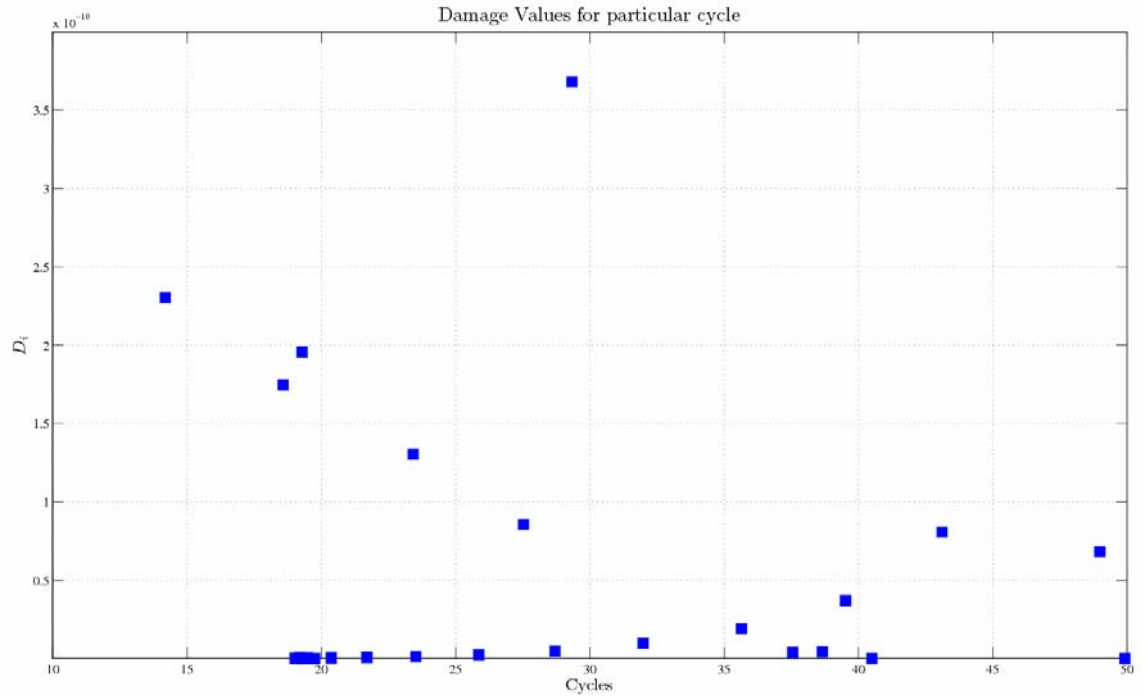

Figure-9. Damage values for the particular cycles.

Where k is the number of cycles that are calculated from the random loading history? Considering the N events per year of normal operating conditions of the WT the estimated accumulated damage for a span of 20 years of service life is given by

$$D_{20} = N * D \quad (26)$$

In the current investigation the number of events of the voltage sags per year is considered to 10. The expected life time T considering the voltage sags that are

estimated from the accumulated damage D that caused by the distinguished cycles in time interval of T_0 is given by.

$$T = \frac{T_0}{D_{20}} \quad (27)$$

From the summary of investigations and the calculations there is expected impact on the current fatigue life considering the grid disturbances shows a considerable reduction, around 10%, of the fatigue life is expected.

CONCLUSIONS

In this paper, the torque transients that developed in the drivetrain of a WT due to electrical disturbances have been analyzed, for a grid connected, constant speed WT. The quantitative results of this current investigation are not necessarily representative of other WT's [15, 16], since they depend critically on the drive train torsional characteristics, as well as on the generator parameters. However, the simulation results presented provide a clear indication of the effect of various abnormal operating conditions and a comparative evaluation of their severity.

From the current investigation on the detrimental effect of fatigue life due to electrical disturbances a methodology is proposed for determining the fragments of service loading that strongly influencing the material fatigue is a good tool for preparation of fatigue tests on the WT system at the early designing stage. This approach can be extended to study the effect of electrical disturbances on drivetrain system in component wise by estimating loading history and their registered service histories which help to have a better design and test setup considerations or while preliminary preparation for further processing. A shortened service history has the same frequency characteristic as the service history, and it is an important advantage of the method.

Appendix-1

1. Drivetrain Specifications used in Simulation

Ratio	1:84.3
Mechanical power	1800 kW

2. Generator Specifications used in Simulation

Rated power	1650 kW
Slip at rated power S_N	0.0117
Voltage U_N	3 x 600 V

The considered generator parameters in p.u. are R_s = 0.048, L_s = 0.1248, R_r = 0.0044, L_r = 0.1791

REFERENCES

[1] Wind Turbine Data Summary Table-2. 2003-2006. Wind Stats Newsletter. 16-19(1-4). 2007. 20(1).

[2] C. Walford. 2006. O and M Cost Model Quantifying the Influence of Reliability, Wind Turbine Reliability Workshop. Global Energy Concepts Seattle, WA. cwalford@globalenergyconcepts.com.

[3] C. Jauch, J. Matevosyan, T. Ackerman, S. Bolik. 2005. International comparison of requirements for connection of wind turbines to power systems. Wind Energy. 8(3).

[4] 2007. Spanish Royal Decree RD 661/2007. BOE.

[5] 2007. German Transmission Code, Vdn.

[6] H. Klee, Simulation of Dynamic Systems with MATLAB and Simulink. CRC Press.

[7] D. W. Novotny, T. A. Lipo. 1996. Vector Control and Dynamics of AC Drives. Oxford: Clarendon Press.

[8] J. F. Manwell, J.G. Mc Gowan, A.L. Rogers. 2002. Wind Energy Explained: Theory, Design and Application. Chichester, NY: Wiley.

[9] H. Baruh. 1999. Analytical dynamics. McGraw Hill.

[10] R. A. Tenenbaum. 2004. Fundamentals of applied dynamics. Springer-Verlag.

[11] H. J. Bollen Math. 2000. Understanding Power Quality Problems: Voltage Sags and Interruptions. New York: IEEE Press/Wiley-Interscience.

[12] 1999. IEC 61400-1, Wind Turbine Generator Systems- Part 1: Safety Requirements, 2nd Edition.

[13] 2007. Standard IEEE-493-2007 (Chapter 7).

[14] 1999. ASTM E 1049-85, 1997, Standard practices for cycle counting in fatigue analysis. Annual Book of ASTM Standards. 3(1): 710-718. Philadelphia.

[15] R. Fadaeinedjad, G. Moschopoulos. 2008. Investigation of Voltage Sag Impact on Wind Turbine Tower Vibrations. Wind Energy. 11(4).

[16] J. Martinez-García, J.A. Dominguez-Navarro. 2008. Behaviour Improvement during Faults of Fixed Speed Stall Control Induction Generator Wind Turbines. Wind Energy. 12(6).